Iran J Sci Technol Trans Civ Eng (2019) 43 (Suppl 1):S331–S341
https://doi.org/10.1007/s40996-018-0168-2

RESEARCH PAPER

Effect of Different Sands on One-Dimensional and Hydraulic Consolidation (Radial) Tests of Clay

Nazile Ural[1] · Burak Görgün[1]

Received: 30 March 2016 / Accepted: 10 September 2018 / Published online: 21 September 2018

Abstract
In settlement problems, the soil type is generally determined by the sand, silt and clay contents. Sieve analysis considers only the percentage of sand, and the grain shape of the sand is ignored. Specifically, sand grains with different characteristics are considered a single type of sand. In this study, variations in the pore size distribution of clay associated with sand particles of different shapes are investigated via consolidation tests. For this purpose, mixtures containing 10%, 20%, 30% and 40% of the two types of sand additions to clay were obtained. Samples of reconstituted clay were prepared using the slurry deposition method. One-dimensional consolidation and radial consolidation (with drainage radially outwards) tests were performed on the samples, and the relationship between the pore size distributions of the mixtures and the consolidation tests was examined. In addition, the mixtures were analysed using helium pycnometry, X-ray diffraction, mercury intrusion porosimetry, Brunauer–Emmett–Teller surface area analysis and scanning electron microscopy.

Keywords Consolidation · Mineralogy · Pore size distribution · Microstructure

1 Introduction

As a whole or in part, soil consists of a binder material that is not cemented, various types of minerals, organic residues, and a mixture of water and air. Soils have undergone a long geological process to reach their present-day state. This process consists of weathering, transport, deposition, freeze–thaw cycles and temperature changes, as well as plant and animal activities. The structure and properties of soil are the result of these processes and other events that have occurred during geologic history. Many studies have been performed on the structure of both natural and artificially prepared soil samples (Tanaka and Locat 1999; Romero et al. 1999; Penumadu and Dean 2000; Mitchell and Soga 2005). These studies state that the microstructural differences in soils are due to the binding between particles (Burland 1990; Liu and Carter 1999). Microstructural properties are known to influence the relative strength of the soil attraction force between particles (Mitchell 1992). However, without considering other factors, the microstructural properties of soil fail to account for its behaviour. The mineralogy, pore size distribution, specific surface area, cation exchange capacity and microstructure of soils directly affect their physical and mechanical properties.

According to one interpretation, the geotechnical properties of clays affect their physico-chemical properties, such as the mineralogy and cation exchange capacity. Additionally, the geotechnical properties of clay sands affect the stiffness of particles with different origins and diameters, as the structure of the spaces that form affects the size distribution. Mahmood and Mitchell (1974) studied the relationship between the constituent materials and the mechanical behaviour of an artificially prepared basalt with silty sand-sized grains and different constituents. They indicated that the crushed basalt was susceptible to different grain arrangements and pore size distributions when deposited in different ways. Holtz and Kovacs (1981) reported that the soil texture can be damaged by stress, and the textures of the grains and pores that are formed may change when compressed. Delage and Lefebvre (1984)

✉ Nazile Ural
nazile.ural@bilecik.edu.tr

Burak Görgün
burak.gorgun@bilecik.edu.tr

[1] Department of Civil Engineering, Bilecik Seyh Edebali University, 11210 Bilecik, Turkey

studied the composition of Champlain clay during consolidation by conducting mercury intrusion porosimetry (MIP) and scanning electron microscopy (SEM) experiments, and they observed that the small pores remained unchanged but that the largest pores collapsed. In another study, the relationship between the structure and consolidation behaviour was investigated. At the end of the study, the macropores decreased in abundance, thereby decreasing the soil permeability (Griffiths and Joshi 1989). Griffiths and Joshi (1991) investigated several clayey soils, and the amount of secondary consolidation varied. Notably, pore size changes from 100 to 10,000 nm were observed during secondary consolidation.

A study by Tanaka et al. (2003) reported the pore size distributions of natural clayey soils around the world. They applied a constant rate of consolidation to both natural and artificial clays and observed that with increasing depth, the diameter of the main pores in the soil decreased; however, some samples did not follow this trend. Accordingly, the pore size distribution, as well as the consolidation pressure, soil index properties, mineralogy and grain size distribution, varied depending on several environmental factors. In another study, consolidation behaviours of undisturbed and reconstituted samples of a fine alluvial clayey soil were investigated. At the end of the study, researchers said that the relationship between the void ratio and vertical effective stress on Shiraz fine soil can be simulated using constitutive equations (Memarzadeh et al. 2017).

Generally, in the literature, artificial samples in the laboratory have been prepared by dry pluviation, wet tamping, sedimentation and slurry deposition. Wet tamping is often performed because of its simplicity. However, in general, sands that contain fines are used in the sedimentation and slurry deposition processes. The method known as slurry deposition is commonly used for fine-grained samples containing more than 20% fine (Kuerbis and Vaid 1988). In this method, soil and water are mixed, and the mixture is poured into a mould. The advantages of the slurry deposition method include the rapid preparation of saturated samples, the use of water to control grain separation, the ability to prepare loose samples, and the ability to grade fine content, regardless of the homogenous void ratio. In this study, the slurry deposition method was chosen to effectively represent important fillings and viaducts and address the problems presented by clayey soils.

Mixtures containing 10%, 20%, 30% and 40% of two different sand additions combined with clay were obtained. The obtained reconstituted clay samples were prepared using the slurry deposition method, and one-dimensional consolidation tests and radial consolidation (with drainage radially outwards) tests were conducted. In addition, the microstructural properties of the soil were investigated to reveal its engineering properties using X-ray diffraction (XRD), MIP, Brunauer–Emmett–Teller (BET) surface area analysis and SEM. Thus, the relationship between the consolidation properties and microstructure of the soils was examined.

2 Materials and Sample Preparation

2.1 Materials

The properties of the clay and the S and M sands used in the tests are given in Table 1. In the experiments, S sand was provided by a commercial company, and M sand was provided by a quarry [the M sand was used after sieving (1–0.074 mm)]. The grain size distribution of the materials is shown in Fig. 1.

2.2 Preparation of the Mixtures

The mixed soils were prepared using 10%, 20%, 30% and 40% dry weights of the S/M sands added to clay. Consistency limit (liquid limit and plastic limit) and specific gravity tests were performed to determine the physical properties of the mixtures. In Table 2, the index properties and the names of the mixtures are provided. Casagrande's method for the liquid limit and the helium pycnometer method for specific gravity were used.

2.3 Preparation of the Samples

In this paper, soil samples prepared by the slurry deposition method were consolidated. According to this method, the dry sample was thoroughly mixed with distilled water at 1.5 times its liquid limit and allowed to stand for 24 h. This mixture was then poured into a cell measuring 7 cm in diameter and 12 cm in height and allowed to stand overnight before starting the consolidation process, which was implemented by loading the sample in increments to reach the prescribed pressure of 50 kPa. Drainage was provided at the top and bottom of the soil.

Table 1 Index properties of clay, S and M sands

Materials	LL (%)	PL (%)	Gs	Classification
Clay	57	28	2.57	CH
S sand	–	–	2.64	SP
M sand	–	–	2.67	SP

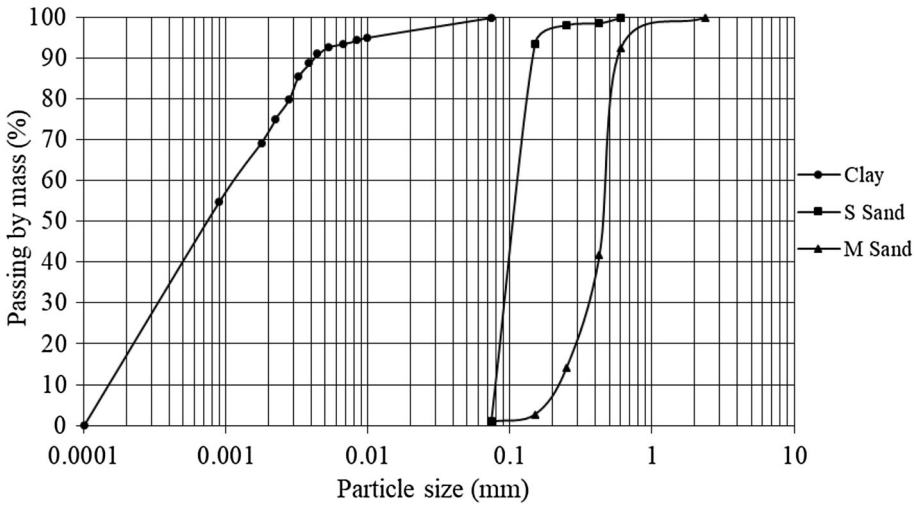

Fig. 1 Grain size distribution of clay, S and M sands

Table 2 Index properties of mixtures

Mixtures name	Additional name of sand	Percentage of the additional sand	LL (%)	PL (%)	Specific gravity (g/cm^3)
C10S	S sand	10	48	28	2.57
C20S	S sand	20	47	27	2.58
C30S	S sand	30	34	25	2.59
C40S	S sand	40	32	24	2.60
C10M	M sand	10	48	28	2.57
C20M	M sand	20	47	27	2.58
C30M	M sand	30	37	26	2.59
C40M	M sand	40	33	24	2.60

3 Methods

3.1 Consolidation Tests

Consolidation is defined by the volume change in saturated soils caused by the dissipation of pore water due to loading. In sandy soils, elevated pore pressure rapidly dissipates the pore water due to the high soil permeability. In clayey soils, elevated pore pressure slowly dissipates the pore water due to low permeability. One-dimensional consolidation (using an oedometer) and hydraulic consolidation (using a Rowe consolidation cell) procedures were implemented for the mixtures. In both experiments, the vertical loads and void ratios were recorded. The vertical stress levels applied were 50, 100, 200, 400, 800, 1600, 400, 100 kPa during both of the consolidation tests. Subsequently, the relationship between the pressure and void ratio was determined from the measured data, which were used to determine the coefficient of consolidation. The coefficient of consolidation was determined by two methods: the root of time method and the log-*t* method.

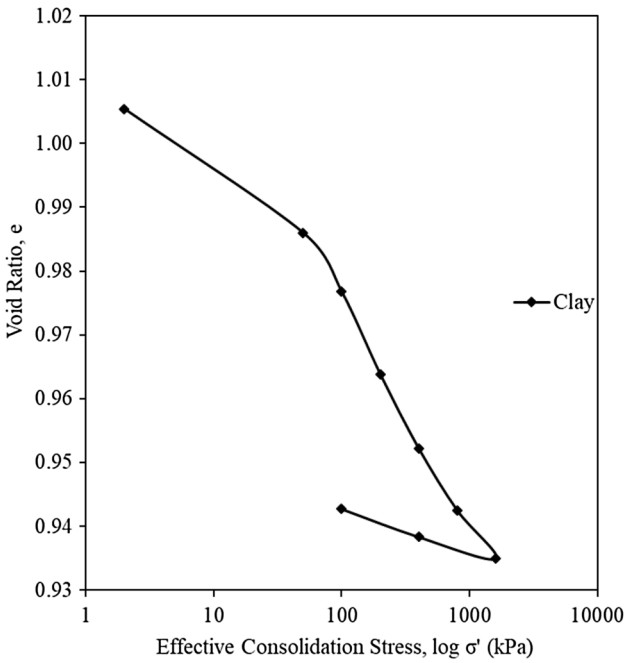

Fig. 2 Void ratio versus effective stress plot (oedometer)

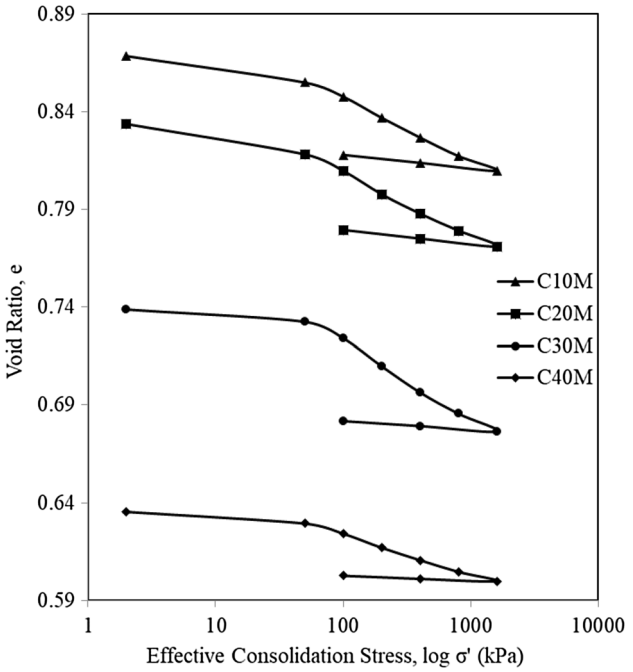

Fig. 3 Results of the oedometer test; C10M, C20M, C30M, C40M, respectively

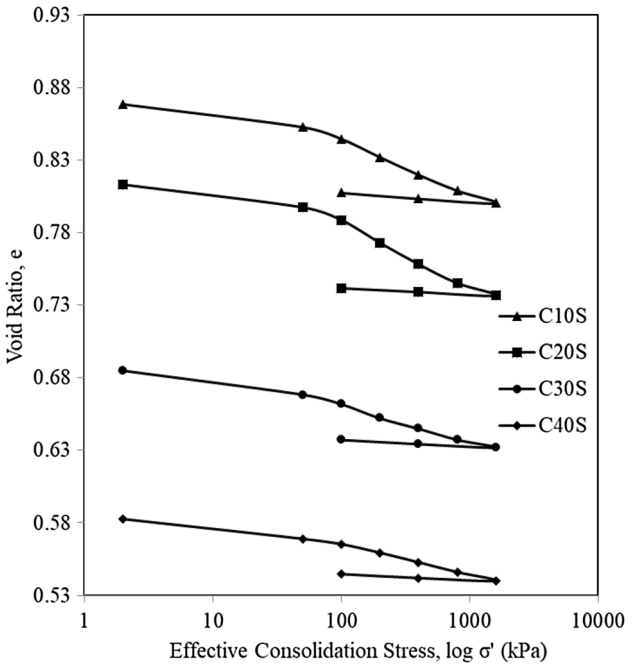

Fig. 4 Results of the oedometer test; C10S, C20S, C30S, C40S, respectively

3.1.1 One-Dimensional Consolidation (Oedometer)

This test was conducted according to ASTM D2435-96 to determine the magnitude and rate of volume decrease for a laterally limited specimen exposed to varying vertical pressures. In this test, a compressive stress is applied to the soil sample by applying a vertical load, and the vertical compression of the soil sample is recorded.

Table 3 Variation of compression index (Cc) and swell index (Cs)

Test	Mixtures name	Cc	Cs
One-dimensional (Oedometer) tests	C	0.0723	0.0092
	C10S	0.0538	0.0062
	C20S	0.0392	0.0055
	C30S	0.0288	0.0038
	C40S	0.0188	0.0029
	C10M	0.0679	0.0077
	C20M	0.412	0.0063
	C30M	0.0307	0.0049
	C40M	0.0197	0.0032
Hydraulic consolidation test (Rowe)	C	0.0554	0.0162
	C10S	0.0505	0.0134
	C20S	0.0481	0.0098
	C30S	0.0442	0.0092
	C40S	0.0395	0.0086
	C10M	0.0506	0.0123
	C20M	0.0482	0.0098
	C30M	0.0434	0.0090
	C40M	0.0357	0.0086

Table 4 Coefficient of consolidation obtained from one-dimensional consolidation

Materials	Cv (cm^2/min)	
	T_{50}	T_{90}
C	0.0105	0.0044
C10S	0.0133	0.0049
C20S	0.0151	0.0066
C30S	0.0173	0.0079
C40S	0.0201	0.0099
C10M	0.0150	0.0066
C20M	0.0173	0.0079
C30M	0.0201	0.0090
C40M	0.0236	0.0109

3.1.2 Hydraulic Consolidation Test (Rowe)

The measurement of one-dimensional consolidation has been improved to overcome previous shortcomings (Rowe and Barden 1966) with the development of hydraulic consolidation tests, which can be used to implement various types of vertical and radial consolidation procedures. In this experiment, the pore water pressure can be measured, drainage can be controlled and a back pressure can be applied to the sample. Radial consolidation tests with

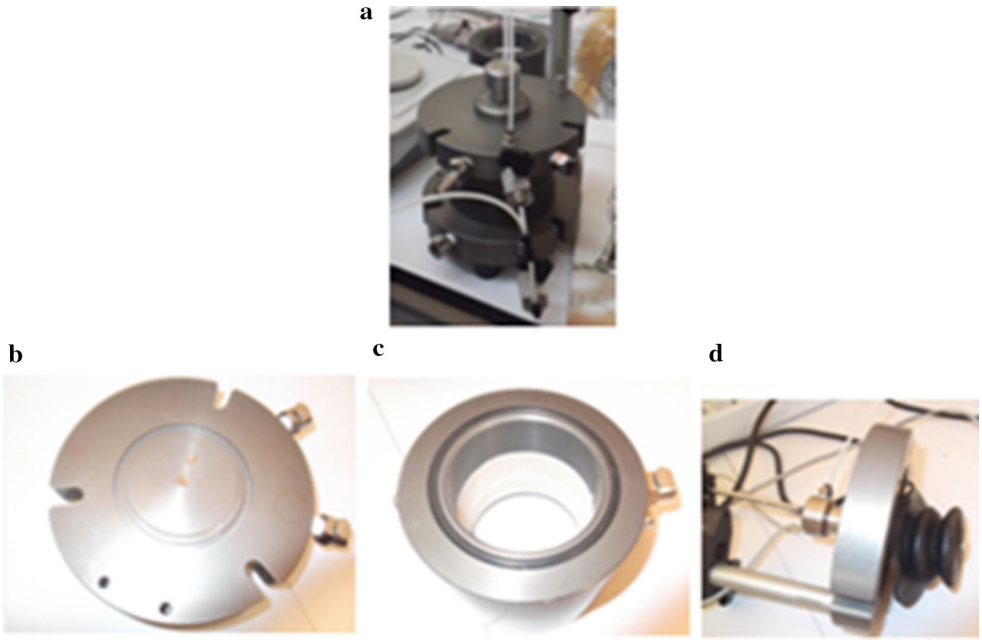

Fig. 5 Rowe cell **a** radial consolidation system **b** bottom plate **c** allowing horizontal drainage cell **d** top plate

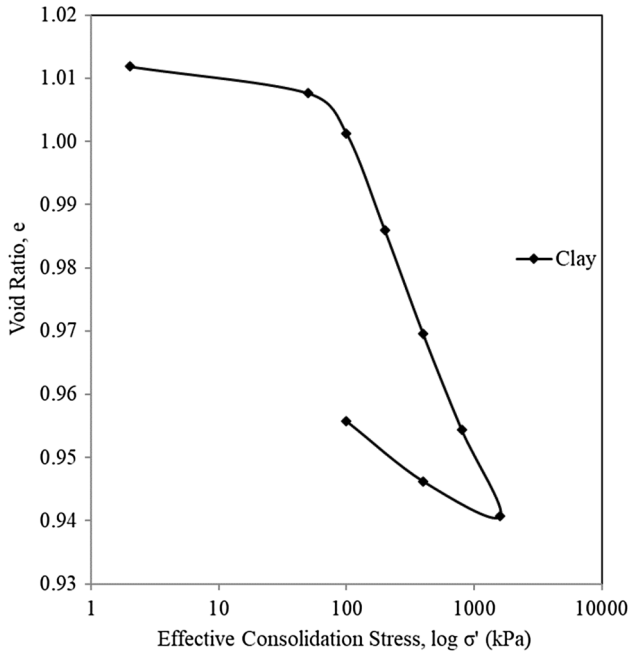

Fig. 6 Void ratio versus effective stress plot (hydraulic consolidation)

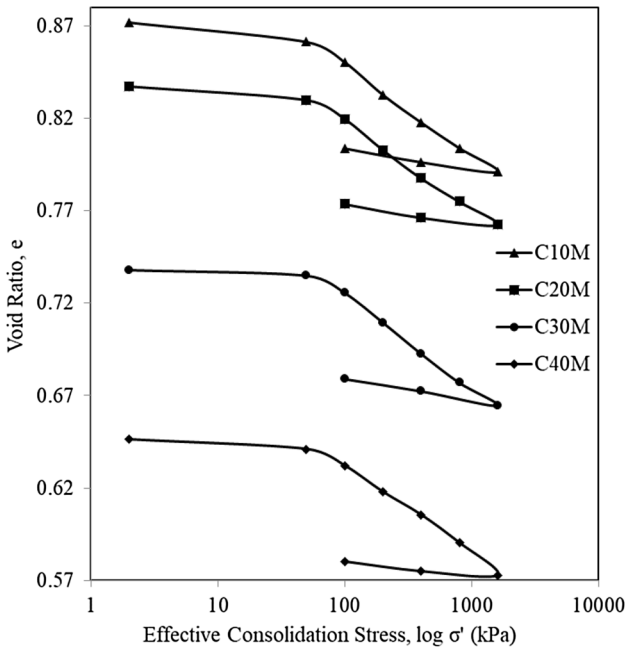

Fig. 7 Results of the hydraulic consolidation test; C10M, C20M, C30M, C40M, respectively

inward or outward drainage can be conducted. In this study, hydraulic consolidation was performed with outward drainage. Hydraulic consolidation tests were conducted according to BS 1377-6:1990, and the load on the samples was applied by an automatically controlled system.

3.2 Physico-chemical Analysis

A soil contains three phases: solid, liquid and gas. The relationships among these three phases are affected by the engineering properties of the soil based on their geological histories. In addition, the sizes of soil grains and the water in pores affect the engineering properties of soils. Researchers have examined the microstructures of soils for

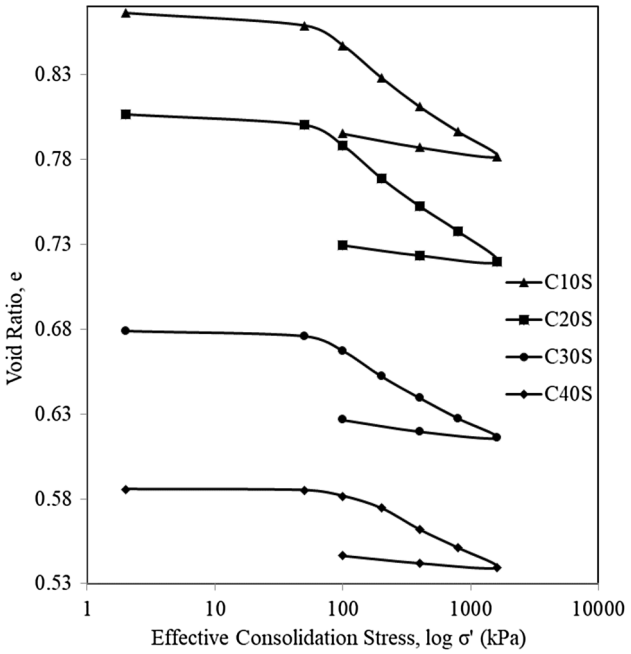

Fig. 8 Results of the hydraulic consolidation test; C10S, C20S, C30S, C40S, respectively

Table 5 Coefficient of consolidation obtained from hydraulic consolidation

Materials	C_r (cm^2/min)	
	T_{50}	T_{90}
C	0.0344	0.0438
C10S	0.0351	0.0486
C20S	0.0377	0.0512
C30S	0.0407	0.0572
C40S	0.0528	0.0725
C10M	0.0399	0.0520
C20M	0.0415	0.0575
C30M	0.0426	0.0613
C40M	0.0452	0.0650

nearly 50 years with advances in microscopy and computer technology. This analysis was conducted using XRD, MIP, BET and SEM to examine the microstructural properties of all the soil samples.

3.2.1 X-ray Diffraction (XRD)

XRD is a quantitative analysis method that uses the powder or mineral content of solid particles with a certain form to provide information, and the various mineral phases in the soil can be observed at the end of the analysis. The mineralogical analysis of soils is very important for geotechnical engineering.

3.2.2 Mercury Intrusion Porosimetry (MIP)

The pore size distribution (PSD) is an important and fundamental parameter that influences the geotechnical behaviour of soil. MIP is a widely used technique to determine the pore size and PSD of bulk soils and powders. In this study, the PSD and the cumulative pore volume are determined based on this method.

3.2.3 Surface Area Analysis Using the BET Method

In civil engineering, experimentally determining the specific surface area of a soil is often preferred. The BET apparatus, which uses solid or powder samples, employs a physical adsorption method to determine the surface area.

3.2.4 Scanning Electron Microscopy (SEM)

SEM produces images of samples by scanning them with a focused beam of electrons. In particular, the microstructure of a soil can be observed using SEM.

4 Experimental Results

The mixed soils were prepared using 10%, 20%, 30% and 40% of the S/M sands (dry weight) added to clay. Tests of the consistency limits (liquid limit and plastic limit) and specific gravity were performed to determine the physical properties of the mixtures. The sample mixtures used to determine the liquid limits were prepared using the slurry deposition method. Then, one-dimensional consolidation (oedometer) and hydraulic consolidation (Rowe) tests were conducted on these samples, as were XRD, MIP, BET and SEM analyses.

4.1 Results of Consolidation Tests

4.1.1 One-Dimensional Consolidation Test (Oedometer)

The vertical deformation of the samples was recorded during this test, and the relationship between the void ratio and the effective stress was determined from the plot in Fig. 2, which presents the results of a typical test. Figure 3 shows that the void ratio versus log effective stress curve trends downward with increasing M-sand percentage during the one-dimensional consolidation test. Figure 4 shows that the same curve trends downward with increasing S-sand percentage. The void ratio versus log effective stress curves for samples with mixtures of S sand are below the those for samples with mixtures of M sand. C10M/S and C20M/S are extremely close together, but C30M/S and C40M/S are separated from each other. Two slopes of

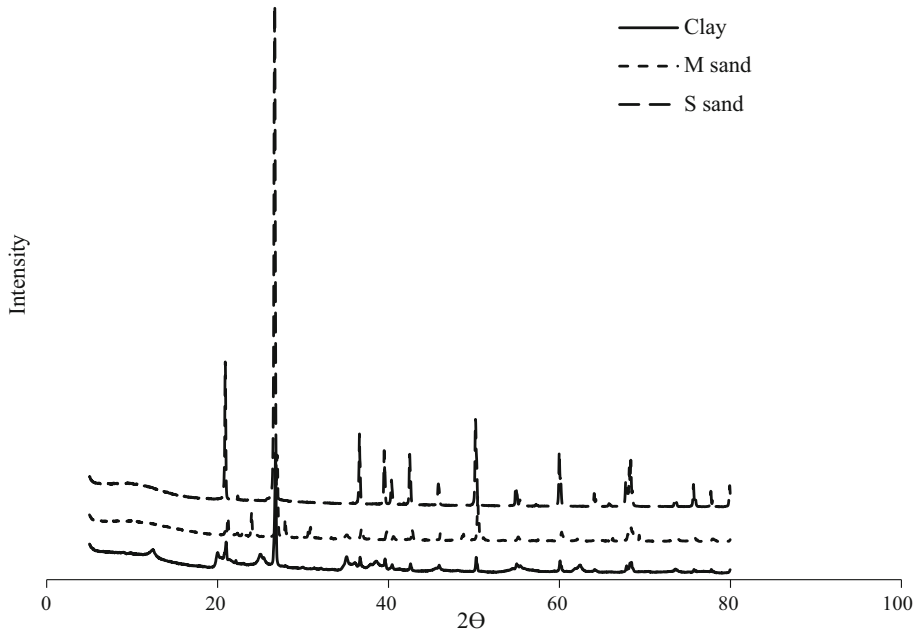

Fig. 9 XRD patterns of clay, S and M sands

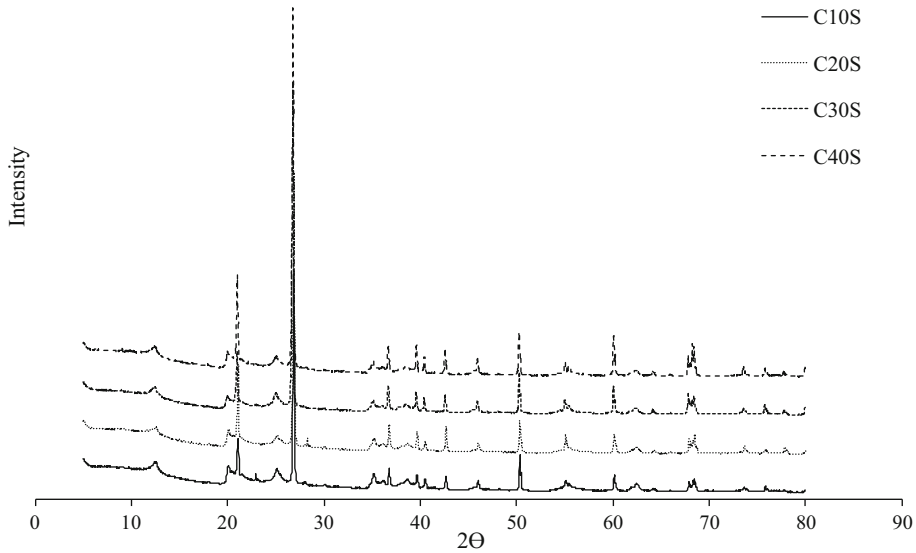

Fig. 10 XRD patterns of C10S, C20S, C30S, C40S, respectively

primary consolidation are defined for the void ratio versus log effective stress curves. First, the compression index is defined as the slope of the compression portion of the e-log p curve. Second, the swell index is defined as the slope of the reload portion the e-log p curve. The compression index (Cc) and swell index (Cs) are given in Table 3. In Table 4, the CV value is shown according to the root of time method and the log-*t* method. This table shows that the coefficient of consolidation increases with increasing sand percentage. The coefficients of consolidation of samples containing mixtures of S sand are much lower than those of samples containing mixtures of M sand.

4.1.2 Hydraulic Consolidation Test (Rowe)

The vertical deformation of the samples was recorded during the test. The relationship between the void ratio and the effective stress was determined from the plot. The hydraulic consolidation apparatus that was used in this study is depicted in shown in Fig. 5. In this study, at the end of each stress period, drainage occurred from the centre outward. This apparatus consisted of a bottom plate, which allowed horizontal drainage, and a top plate. Figure 6 presents the results of a typical test, and Fig. 7 shows that the void ratio versus effective stress curve trends downward as the M-sand percentage increases in the

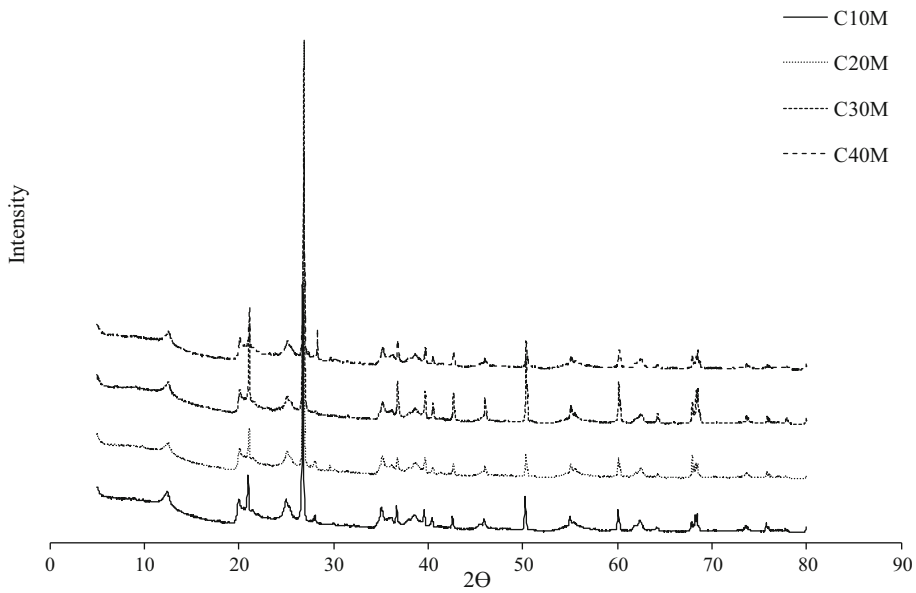

Fig. 11 XRD patterns of C10M, C20M, C30M, C40M, respectively

hydraulic consolidation test. Figure 8 shows that the same curve trends downward with increasing S-sand percentage in the hydraulic consolidation test. As indicated by these curves, the initial void ratio of the samples is between 0.56 and 0.90. The void ratio versus effective stress curves of the samples containing mixtures of S sand are below those of samples with mixtures of M sand. C10M/S and C20M/S are extremely close together, but C30M/S and C40M/S are farther apart. In Table 5, the CV value is shown according to the root of time method and the log-*t* method. This table shows that the coefficient of consolidation increases with increasing sand percentage. The coefficients of consolidation for samples with mixtures of S sand are much lower than those for samples with mixtures of M sand.

4.2 Results of the Physico-chemical Analysis

4.2.1 X-ray Diffraction (XRD) Analysis

In this analysis, X-rays from very short-length electromagnetic waves are reflected onto the atoms of the crystals. The X-rays pass through the powder sample, which is rotated at a certain angle, so that reflection occurs. Traces of the reflected rays are detected on the photo card. The well-known standard minerals are used for the determination of sample mineralogy. Figure 9 gives the XRD results for clay and sands. The XRD patterns of the clay indicate the presence of kaolinite, whereas the XRD patterns of the S and M sands reflect the presence of quartz. The XRD results for all the samples are given in Figs. 10 and 11, which show that the XRD patterns of the mixed S/M sand samples indicate the presence of quartz and kaolinite.

4.2.2 Mercury Intrusion Porosimetry (MIP)

Figure 12 illustrates the PSDs of the mixed S and M sand samples. The changes in the pore volumes and the pore size diameters of the samples mixed with S/M sand are given in this figure, which shows that the cumulative pore volume decreased with increasing sand percentage for 30% sand and then increased again. This trend suggests increased contact between the sand particles and the reduced effect of the clay with increasing sand percentage.

4.2.3 BET Surface Area Analysis

The specific surface areas obtained are given in Table 6, which shows that the specific surface area decreased with increases in both the S- and M-sand percentages.

4.2.4 Scanning Electron Microscopy (SEM)

The SEM analyses of clay are shown in Fig. 13a (10.000× magnification), and the SEM analyses of S and M sands are given in Fig. 13b (100× magnifications). The SEM images of all the samples are given in Figs. 14 and 15 (10.000× magnifications). These figures show more dispersed structures with increasing sand percentages. When comparing both of the sand mixtures, fewer pores are found in the structures of the samples mixed with S sand than in the other samples.

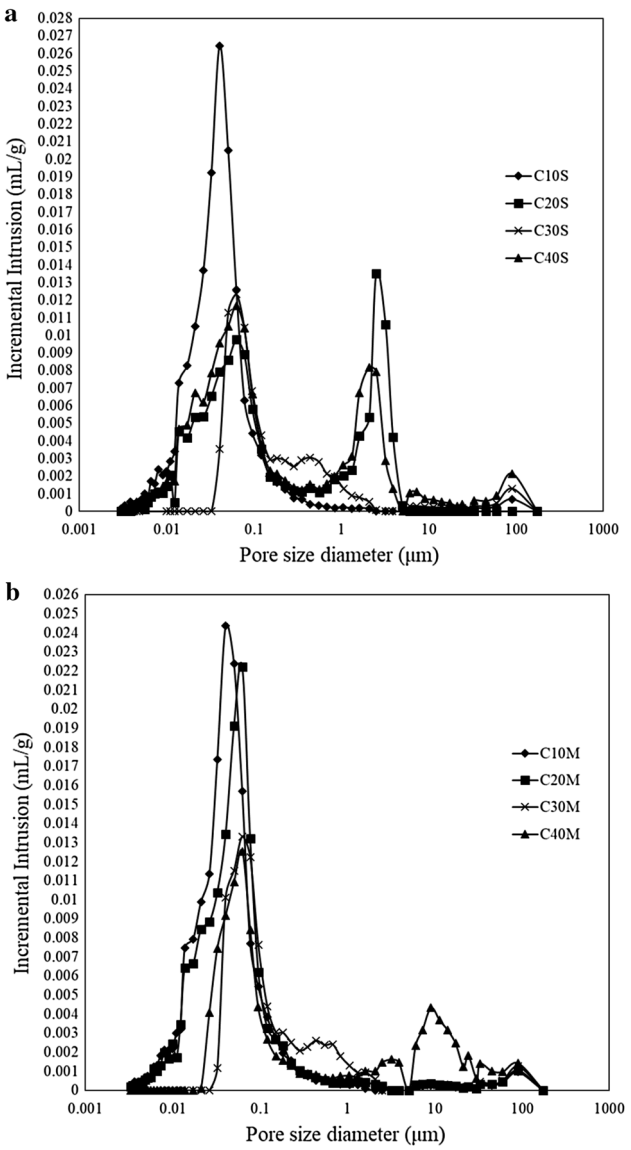

Fig. 12 Pore size distribution of samples mixed with sands measured by mercury intrusion porosimetry **a** with S sand **b** with M sand

Table 6 Specific surface area (BET)

Materials	Specific surface area (BET) (m^2/g)
C	24.122
C10S	21.686
C20S	19.565
C30S	16.839
C40S	14.789
C10M	21.720
C20M	19.858
C30M	17.361
C40M	15.251

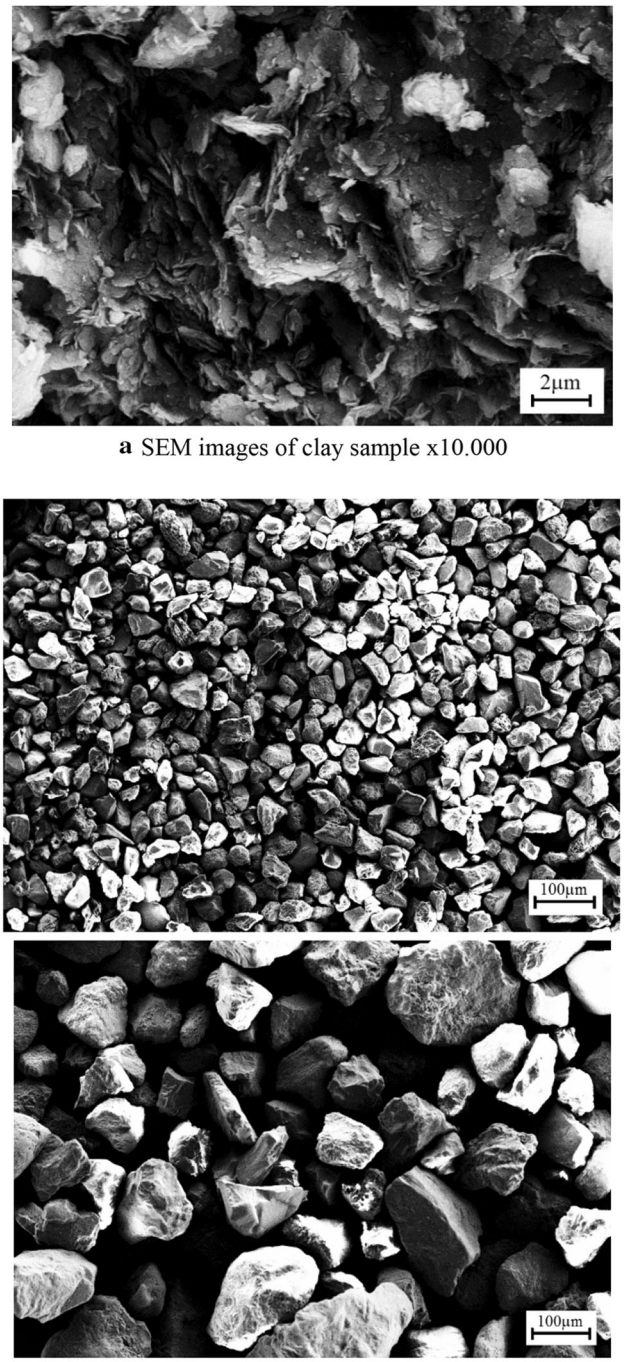

a SEM images of clay sample x10.000

b SEM images of S and M sands x100

Fig. 13 SEM images of materials. **a** SEM images of clay sample ×10.000, **b** SEM images of S and M sands ×100

5 Conclusions

In this study, one-dimensional consolidation and radial consolidation (with drainage radially outwards) tests were conducted for mixed sand and clay samples. Mixtures containing 10%, 20%, 30% and 40% of the two types of

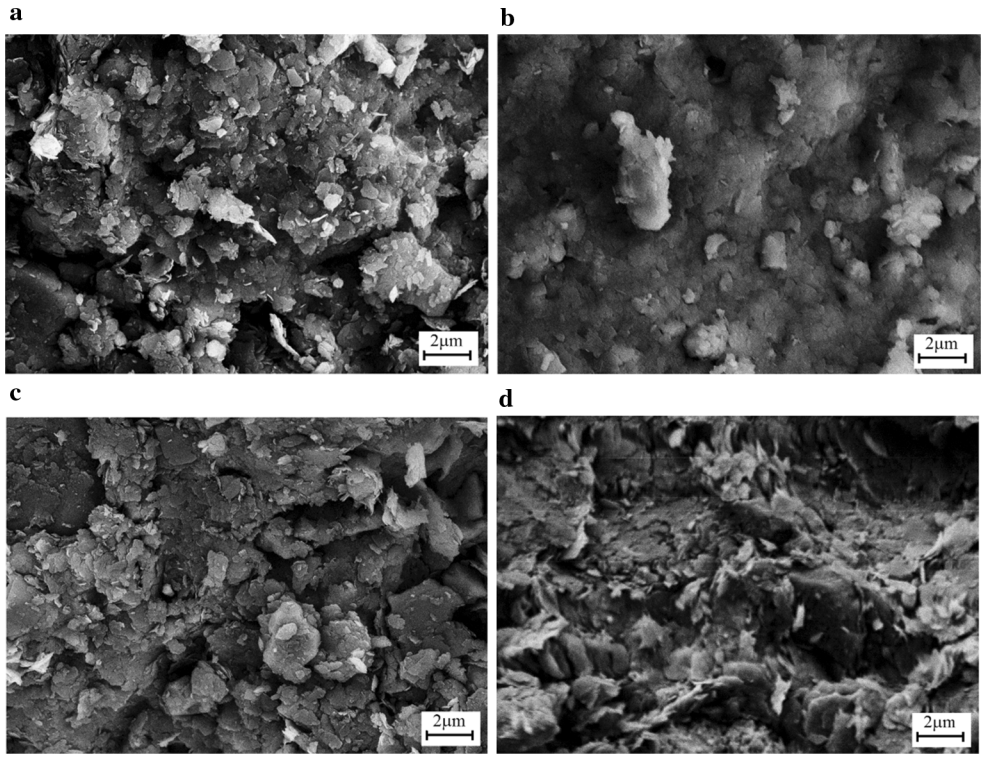

Fig. 14 SEM images (×10,000) **a** C10S, **b** C20S, **c** C30S, **d** C40S

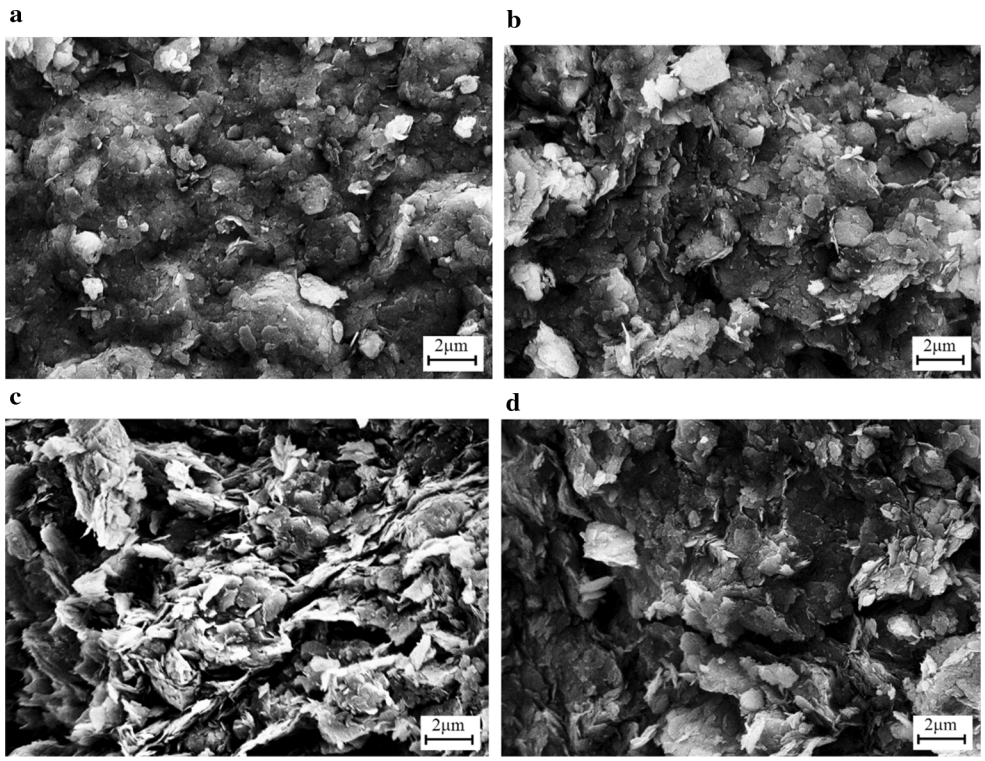

Fig. 15 SEM images (×10,000) **a** C10M, **b** C20M, **c** C30M, **d** C40M

sand that were added to clay and reconstituted samples that were prepared by the slurry deposition method were obtained. After the completion of the experiments, the effect of the clay on the PSD due to the shapes of sand particles in the consolidation test was examined. In addition, the mixtures were analysed using helium pycnometry, XRD, MIP, BET and SEM. The following conclusions were drawn based on the test results and the discussion presented in this study.

- In the one-dimensional consolidation test, the void ratio–stress curve exhibited a downward trend with the addition of sand. The coefficient of consolidation increased with the addition of both sands. However, this increase was smaller for the S sand samples than for the M sand samples.
- In the hydraulic consolidation test, the void ratio–stress curve displayed a downward trend with the addition of sand. The consolidation coefficient increased with the addition of both sands. However, this increase was smaller for samples with S sand than for those with M sand.
- When the two consolidation tests were compared, the void ratio and the effective stress curves from the one-dimensional consolidation tests covered a wider range than those from the hydraulic consolidation tests.
- For certain sand percentages, the cumulative pore volume decreased with increasing sand percentage. However, after a certain sand percentage was reached, the cumulative pore volume increased again with increasing sand percentage. Lower values were observed in S sand than in M sand.
- The cumulative pore volume did not cause a decrease or increase in the coefficient of consolidation. However, the void ratio versus effective stress curve of the sample with 30% sand was below those of the samples with 10% and 20% sand. Additionally, the curve of the sample with 40% sand was lower than that of the sample with 30% sand.
- The flaky appearance of clay varied with the addition of S and M sand. With the addition of sand, the number of voids decreased, and the soil structure became more dispersed.

Acknowledgements The Scientific and Technological Research Council of Turkey (TUBITAK) sponsored research Project 112M575. The authors wish to express their gratitude to The Scientific and Technological Research Council of Turkey for its financial assistance.

References

ASTM D2435-96 Standard test method for one dimensional consolidation properties of soils

BSI 1337-6:1990. Determination of consolidation using a hydraulic cell, methods of test for soils for civil engineering purposes—part 6: consolidation and permeability tests in hydraulic cells and with pore pressure measurement. British Standard

Burland JB (1990) On the compressibility and shear strength of natural clays. Géotechnique 40(3):329–378

Delage P, Lefebvre G (1984) Study of the structure of a sensitive champlain clay and of its evolution during consolidation. Can Geotech J 21:21–35

Griffiths FJ, Joshi RC (1989) Change in pore size distribution due to consolidation of clays. Geotechnique 39(1):159–167

Griffiths FJ, Joshi RC (1991) Change in pore size distribution owing to secondary consolidation of clays. Can Geotech J 28:20–24

Holtz RD, ve Kovacs WD (1981) An introduction to geotechnical engineering. Prentice Hall, Englewood Cliffs

Kuerbis R, Vaid YP (1988) Sand sample preparation—the slurry deposition method. Soils Found 28(4):107–118

Liu MD, Carter JP (1999) Virgin compression of structured soils. Géotechnique 49(1):43–57

Mahmood A, Mitchell J (1974) Fabric property relationship in fine granular materials. Clay Clay Miner 22:397–408

Memarzadeh I, Lashkari A, Shourijeh PT (2017) Consolidation behavior of structured clayey soils: a case study on shiraz fine alluvial strata. Int J Civil Eng 1:1–10

Mitchell JK (1992) Fundamentals of soil behaviour, 2nd edn. Wiley, New Jersey **(Printed in the United States of America)**

Mitchell JK, Soga K (2005) Fundamentals of soil behavior. Wiley, New Jersey

Penumadu D, Dean J (2000) Compressibility effect in evaluating the pore size distribution of kaolin clay using mercury intrusion porosimetry. Can Geotech J 37:393–405

Romero E, Gens A, Lloret A (1999) Water permeability, water retention and microstructure of unsaturated Boom clay. Eng Geol 54:117–127

Rowe PW, Barden L (1966) A new consolidation cell. Geotechnique 16(2):162–170

Tanaka H, Locat J (1999) A microstructural investigation of Osaka Bay clay: the impact of microfossils on its mechanical behaviour. Can Geotech J 36:493–508

Tanaka H, Shiwasoti DR, Omukai N, Rito F, Locat J, Tanaka M (2003) Pore size distribution of clayey soils measured by mercury intrusion porosimetry and its relation to hydraulic conductivity. Soils Found 43(6):63–73